

Hyperfine Structure of the $3d^8 4s^2 {}^3F_2$ Metastable Atomic State of ${}^{61}\text{Ni}$ †

W. J. Childs and B. Greenebaum*

Argonne National Laboratory, Argonne, Illinois 60439

(Received 25 February 1972)

The hyperfine structure (hfs) of the $3d^8 4s^2 {}^3F_2$ metastable atomic state of ${}^{61}\text{Ni}$ has been measured by the atomic-beam magnetic-resonance technique. Isotopic enrichment of the normally 1% abundant ${}^{61}\text{Ni}$ was necessary to achieve adequate intensity. The results, when combined with earlier hfs measurements of the ${}^3F_{4,3}$ states of ${}^{61}\text{Ni}$, allow a comparison with predictions of Bauche-Arnoult's recent theoretical treatment of the effects of configuration interaction on hfs. Good agreement is found. Similar experimental results for the Hund-rule terms of other $3d^N 4s^2$ atoms are tabulated. The electron spin density at the nucleus, as determined from the experimental hfs results, is compared with recent unrestricted-Hartree-Fock calculations.

I. INTRODUCTION

Hyperfine-structure (hfs) measurements in several members of one or more multiplets within a single atomic configuration make possible the study of the relative strengths of the orbital, spin-dipole, contact, and other contributions to the hfs Hamiltonian. Such measurements have been made for several atoms in the $3d$ shell.¹⁻⁸ Investigations have also been made of the variation of some of these contributions from one atom to another within an electronic shell. Examples of this type of comparison may be found in the papers of Winkler⁹ and of Childs,¹⁰ who considered trends in the contribution of core polarization in $3d$ atoms, as inferred from experimental data, and in Bauche-Arnoult's comparison¹¹ between her theoretical predictions and the experimental results for some ratios of the parameters characterizing these strengths in the Hamiltonian.

We have measured the hyperfine-interaction constants in the $3d^8 4s^2 {}^3F_2$ state of ${}^{61}\text{Ni}$. Combining our results with earlier measurements⁶ of the 3F_4 and 3F_3 states enables us to determine the three parameters in the dipole hfs Hamiltonian of Sandars and Beck¹² and to compare the parameters for nickel with several theoretical and empirical results in other $3d$ -shell atoms.

II. EXPERIMENTAL APPARATUS AND OBSERVATIONS

The measurements were made by the conventional atomic-beam magnetic-resonance method,¹³ using virtually the same technique as for the previous nickel experiments.⁶ Previous articles have described both the atomic-beam apparatus¹⁴ and the digital electronic system⁴ used to integrate the weak signal for a long time, in order to separate it from the background.

The only stable nickel isotope that exhibits a hfs is ${}^{61}\text{Ni}$ ($I = \frac{3}{2}$); the natural abundance of this isotope is only 1%. In order to have a sufficiently large

fraction of the atomic beam in the $3d^8 4s^2 {}^3F_2$ state of ${}^{61}\text{Ni}$, we enriched the oven loads to 10% ${}^{61}\text{Ni}$ by combining a piece of the natural metal with some separated ${}^{61}\text{Ni}$ in the form of the powdered metal, purchased from Oak Ridge National Laboratory. An oven load, which consisted of 100 mg of metal, usually produced a steady beam of workable intensity for the better part of a day. Whenever an oven that was producing a good beam was turned off overnight, the beam obtained the next day was not of as good quality. The mass spectrum observed for such an enriched beam is shown in Fig. 1; in the corresponding spectrum for a beam of natural (unenriched) nickel, the number of atoms of mass 61 is about an order of magnitude smaller. The mass-55 contaminant was not investigated, but probably arises from a trace of ${}^{55}\text{Mn}$, which is much more volatile than nickel.

The ovens were closed 0.25-in.-diam cylinders

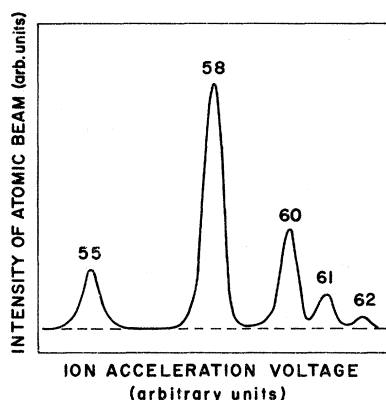


FIG. 1. Mass spectrum observed for the nickel beam enriched to 10% in ${}^{61}\text{Ni}$. The nonbeam background has been subtracted. The component of mass 55 in the beam probably arises from trace impurities of the much more volatile ${}^{55}\text{Mn}$ and was not investigated. The mass-spectrometer slit was set on $A = 61$ for the experiment.

TABLE I. Excitation energies^a and Boltzmann factors for members of the two lowest multiplets in Ni I. The Boltzmann factors are calculated for $T=1700^\circ\text{C}$, at which the vapor pressure is about 0.1 Torr.

Electron configuration	State	Excitation energy ΔE (cm^{-1})	$\exp(-\Delta E/kT)$ ($T=1700^\circ\text{C}$)
$3d^8 4s^2$	3F_4	0.0	1.000
$3d^9 4s$	3D_3	204.8	0.861
$3d^9 4s$	3D_2	879.8	0.527
$3d^9 4s^2$	3F_3	1332.2	0.379
$3d^9 4s$	3D_1	1713.1	0.287
$3d^9 4s^2$	3F_2	2216.5	0.199

^aExcitation energies are taken from *Atomic Energy Levels*, edited by C. E. Moore, Natl. Bur. Std. (U. S.) Circ. No. 467 (U. S. GPO, Washington, D. C., 1952), Vol. II, p. 98.

of stabilized zirconia, with an 0.01×0.25 -in. vertical slit in the wall. The ovens were enclosed in a tantalum jacket, which was heated by electron bombardment to about 1700°C . At this temperature nickel has a vapor pressure of about 0.1 Torr and forms a satisfactory beam. The excitation energies and Boltzmann factors for the two lowest multiplets in Ni I are shown in Table I.

Nine resonances were observed in the 3F_2 state of ^{61}Ni . Resonances for which $\Delta F=0$ were observed in the $F=\frac{7}{2}, \frac{5}{2},$ and $\frac{3}{2}$ states at fields up to 200 G. (Throughout this report the levels in-

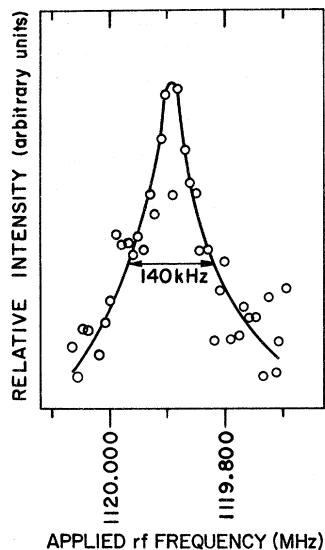


FIG. 2. Appearance of the $(\frac{3}{2}, \frac{1}{2}, \leftrightarrow \frac{5}{2}, -\frac{1}{2})$ transition in the 3F_2 state of ^{61}Ni near $H=1$ G. Excessive rf power was inadvertently applied for this run. In subsequent runs at reduced-power levels, the full width at half-maximum was about 100 kHz and there was no evidence of frequency "pulling".

involved in transitions are identified by the zero-field quantum number F , which characterizes the total angular momentum $\vec{F}=\vec{I}+\vec{J}$, and by its z projection M). These observations were used in a computer optimization program to find preliminary values for the hfs dipole- and quadrupole-interaction constants A and B . The program used the usual Hamiltonian¹⁵ for an atom in an external magnetic field H , namely,

$$\begin{aligned} \mathcal{H} &= \mu_B (g_J \vec{J} + g_I \vec{I}) \cdot \vec{H} + \mathcal{H}_{\text{hfs}}^c(M1) + \mathcal{H}_{\text{hfs}}^c(E2) \\ &= \mu_B (g_J \vec{J} + g_I \vec{I}) \cdot \vec{H} + A \vec{I} \cdot \vec{J} + B Q_{\text{op}}, \end{aligned} \quad (1)$$

where J is the electronic angular momentum (assumed to be a good quantum number), I is the nuclear spin, $-g_J$ and $-g_I$ are the ratios of magnetic moment (in Bohr magnetons) to spin for the electrons and the nucleus, respectively, and the quadrupole operator is

$$Q_{\text{op}} = \frac{\frac{3}{2} \vec{I} \cdot \vec{J} (2\vec{I} \cdot \vec{J} + 1) - I(I+1)J(J+1)}{2I(2I-1)J(2J-1)}. \quad (2)$$

The preliminary values of A and B were used to define a reasonable search range for $\Delta F=1$ transitions, and two of these were observed. The value of the homogeneous magnetic field H for each nickel resonance was measured by observing a resonance in ^{39}K before, during, and after each data run. Figure 2 shows the appearance of the $(\frac{3}{2}, \frac{1}{2} \leftrightarrow \frac{5}{2}, -\frac{1}{2})$ resonance at $H \approx 1$ G. All of the nickel resonances were used to make a final computer fit to A , B , and g_J ; in this fit the value of the nuclear moment was held fixed at $-0.7487 \mu_N$, as measured by nuclear magnetic resonance.¹⁶ Table II summarizes all our observations and lists the residual for each run as found from the final least-squares fit, after the corrections outlined below have been applied.

TABLE II. Summary of the observed transition frequencies in the $3d^8 4s^2 ^3F_2$ state of ^{61}Ni . The last column shows the differences between the observed resonance frequencies and the frequencies calculated from Eq. (1) by use of the final values of A , B , C , and g_J listed in the last column of Table III.

H (G)	Observed frequency (MHz)	Transition ($F, M \leftrightarrow F', M'$)	$\nu_{\text{obs}} - \nu_{\text{calc}}$ (kHz)
20	10.752(12)	$\frac{7}{2}, \frac{5}{2} \leftrightarrow \frac{7}{2}, \frac{1}{2}$	24
50	26.957(11)	$\frac{7}{2}, \frac{5}{2} \leftrightarrow \frac{7}{2}, \frac{1}{2}$	15
100	60.724(15)	$\frac{5}{2}, \frac{3}{2} \leftrightarrow \frac{5}{2}, \frac{1}{2}$	-4
100	54.218(5)	$\frac{7}{2}, \frac{5}{2} \leftrightarrow \frac{7}{2}, \frac{1}{2}$	-26
200	108.960(10)	$\frac{7}{2}, \frac{3}{2} \leftrightarrow \frac{7}{2}, \frac{1}{2}$	6
200	125.305(10)	$\frac{5}{2}, \frac{3}{2} \leftrightarrow \frac{5}{2}, \frac{1}{2}$	9
200	165.162(10)	$\frac{3}{2}, \frac{1}{2} \leftrightarrow \frac{3}{2}, -\frac{1}{2}$	2
1.023	1119.890(22)	$\frac{3}{2}, \frac{1}{2} \leftrightarrow \frac{3}{2}, -\frac{1}{2}$	0
1.000	1634.022(15)	$\frac{5}{2}, \frac{3}{2} \leftrightarrow \frac{5}{2}, \frac{1}{2}$	0

Table III shows the results of the computer fit for the interaction constants of the 3F_2 state, as obtained by use of the Hamiltonian of Eq. (1); this table also includes the $3d^8 4s^2 {}^3F_3$ and 3F_4 results of the previous experiment.⁶

III. CALCULATION OF hfs INTERACTION PARAMETERS

The physical states to which the Hamiltonian in Eq. (1) is applied are linear combinations of the pure L - S basis states arising from the $3d^8 4s^2$ configuration and possibly from other configurations as well. The earlier work of Childs, Fred, and Goodman⁶ reports a fit to the observed energies of 41 levels in NI I in five configurations. They used 19 parameters and report an average error of 21 cm^{-1} in the energies, which ranged up to $55\,000 \text{ cm}^{-1}$. Their eigenvectors gave excellent agreement with their high-precision measurements of the g_J values of seven low-lying states. It is impractical to use such complex eigenvectors for calculation of hfs effects in low-lying levels, however, because the amount of experimental information available is not sufficient to specify all of the relevant parameters.

As a first approximation, a given physical state in an atom with only one partially filled electron shell can reasonably be thought of as being composed only of admixtures of other states within the same configuration. Sandars and Beck,¹² Wybourne,¹⁷ and others have shown that configuration interaction and relativistic effects in the hfs can be accounted for by using effective operators in the hfs Hamiltonian. They introduce the quantities $a(l)$, $a(sC^2)$, and $a(s)$ and allow them to be treated as parameters in the dipole hfs Hamiltonian

$$\mathcal{H}_{\text{hfs}}(M1) = \sum_{i=1}^N [a(l)\bar{1}_i - (10)^{1/2} a(sC^2) \times (\bar{3}C^2)_i^{(1)} + a(s)\bar{3}_i] \cdot \bar{1}. \quad (3)$$

In the case of $3d^N 4s^2$ atoms, it should be noted that the major configuration-interaction effect in the dipole part of the Hamiltonian is through the core polarization¹⁸ of the inner s electrons. This interaction appears in the $a(s)$ term of Eq. (3). For NI I, the low-lying $3d^8 4s$ configuration may also make important contributions to the hfs of the $3d^8 4s^2 {}^3F$ levels. While configuration interaction with other configurations is probably small, the cumulative contribution of such interactions with many configurations could be substantial and may distort the values observed for the dipole parameters. Relativistic effects, though capable of distorting the radial parameters in the hfs Hamiltonians, should play only a very minor role for the light atoms considered in this paper.

The corresponding Hamiltonian for the quadrupole hfs can be written in several equivalent forms, one of which¹⁹ is

$$\mathcal{H}_{\text{hfs}}(E2) = \frac{r_n^2 e^2}{r_e^3} \bar{C}_n^{(2)} \cdot \sum_{i=1}^N \left[\frac{b^{02}}{b_{ni}} \left(\frac{2l(l+1)(2l+1)}{(2l-1)(2l+3)} \right)^{1/2} \bar{U}_i^{(02)2} + \left(\frac{3}{10} \right)^{1/2} \frac{b^{13}}{b_{ni}} \bar{U}_i^{(13)2} + \left(\frac{3}{10} \right)^{1/2} \frac{b^{11}}{b_{ni}} \bar{U}_i^{(11)2} \right], \quad (4)$$

in which b^{02} , b^{13} , and b^{11} are adjustable parameters. The $\bar{U}^{(k_s, k_l)2}$ are double-tensor operators²⁰ associated with the electrons. They have rank k_s in spin space, k_l in orbital space, and 2 in the combined space. The tensor operator associated

TABLE III. Summary of the experimental values of the hyperfine-interaction constants A , B , C , and the electron g factor g_J for the $3d^8 4s^2 {}^3F$ multiplet in ${}^{61}\text{Ni}$. The results for the 3F_3 and 3F_4 states are based on the data of Ref. 6. Values in column 3 result from a least-squares fit to the observed resonances; those in column 5 are for a similar fit that includes corrections for hyperfine and Zeeman interactions between 3F states of different J . The final values (column 5) for 3F_3 and 3F_4 differ slightly from those in Ref. 6, as explained in the text.

State	Parameter	Observed value (MHz)	Off-diagonal hfs correction (MHz)	Final value (MHz)
3F_2	A	-457.185(6)	-0.001	-457.186(6)
	B	-38.011(22)	+0.003	-38.008(22)
	C	(Assumed to be 0; only two intervals measured)		
	g_J	0.66957(3)	-0.00001	0.66956(3)
3F_3	A	-299.312(2)	-0.001	-299.313(2)
	B	-42.071(13)	-0.008	-42.079(13)
	C	(Assumed to be 0; only two intervals measured)		
	g_J	1.08280(3)	0.00000	1.08280(3)
3F_4	A	-215.040(2)	0.000	-215.040(2)
	B	-56.872(18)	-0.004	-56.876(18)
	C	0.000(1)	0.000	0.000(1)
	g_J	1.24964(4)	0.00001	1.24965(4)

with the nucleus is

$$e\gamma_n^2 \overline{C}_n^{(2)} = \overline{T}_n^{(2)}, \quad (5)$$

which is related to the nuclear electric-quadrupole moment Q by the relation

$$\langle I, M_I = I | \overline{T}_n^{(2)} | II \rangle = \frac{1}{2} eQ. \quad (6)$$

In Eq. (4), the second and third terms are entirely relativistic in origin, and in the nonrelativistic limit only the first term remains. In this limit, b^{13} and b^{11} approach zero and b^{02} approaches the nonrelativistic quadrupole parameter

$$b_{nI} = e^2 Q \langle r^{-3} \rangle_{nI}, \quad (7)$$

where

$$\langle r^{-3} \rangle_{nI} = \int_0^\infty |R_{nI}^2| r^{-3} dr. \quad (8)$$

The one-term nonrelativistic Hamiltonian may be expected to be consistent with the quadrupole hfs of the light nickel atom to a high order.

We have formed eigenvectors for the 3F multiplet of Ni I by fitting the observed energies of the nine states in the $3d^3 4s^2$ configuration, using as variables the three Slater parameters F^0 , F^2 , and F^4 and the spin-orbit coupling constant ξ_{3d} . Our eigenvectors are

$$|{}^3F_2^{\wedge}\rangle = 0.996175|{}^3F_2\rangle - 0.087095|{}^1D_2\rangle - 0.007107|{}^3P_2\rangle, \quad (9a)$$

$$|{}^3F_3^{\wedge}\rangle = |{}^3F_3\rangle, \quad (9b)$$

$$|{}^3F_4^{\wedge}\rangle = 0.999467|{}^3F_4\rangle + 0.032635|{}^1G_4\rangle. \quad (9c)$$

In Eqs. (9), the states on the left-hand side are the physical states; those on the right-hand side are the pure L - S basis states. It can be seen that the physical states are fairly close to the L - S limit. For this one-configuration model, the impurities in the ${}^3F_2^{\wedge}$ physical state total only 0.8%; they increase to 4.6% in the multiconfiguration model of Ref. 6.

Using the eigenvectors of Eqs. (9), we find that the A - and B -interaction constants of Eq. (1) are related to the parameters through the expressions

$$A(|{}^3F_4^{\wedge}\rangle) = 0.750266a(l) - 0.042666a(sC^2) + 0.249734a(s), \quad (10a)$$

$$A(|{}^3F_3^{\wedge}\rangle) = 0.916667a(l) + 0.035714a(sC^2) + 0.083333a(s), \quad (10b)$$

$$A(|{}^3F_2^{\wedge}\rangle) = 1.330764a(l) + 0.063600a(sC^2) - 0.330763a(s), \quad (10c)$$

$$B(|{}^3F_4^{\wedge}\rangle) = -0.286627b^{02} - 0.030390b^{13} - 0.195438b^{11} \approx -0.286627b_{3d}, \quad (11a)$$

$$B(|{}^3F_3^{\wedge}\rangle) = -0.214286b^{02} + 0.043741b^{13} - 0.083333b^{11}$$

$$\approx -0.214286b_{3d}, \quad (11b)$$

$$B(|{}^3F_2^{\wedge}\rangle) = -0.190814b^{02} + 0.064174b^{13} + 0.080845b^{11} \approx -0.190814b_{3d}. \quad (11c)$$

Even though the hfs Hamiltonians (3) and (4) have nonzero off-diagonal matrix elements between states of different J in the same configuration,³ the computer-fitting routine is based on Eq. (1), which assumes that J is a good quantum number for the physical states. The corrections to the A , B , C , and g_J values for all three states in the $3d^3 4s^2 {}^3F$ multiplet were calculated and are listed in the next to the last column of Table III. The last column of Table III gives the corrected values for the constants of the three states. The corrections listed for the 3F_3 and 3F_4 states differ in sign from those in Ref. 6 as a result of an error in the previous work; the method of calculation is the same as in Ref. 6. It should be noted, however, that in this multiplet the corrections are somewhat smaller than the experimental uncertainties of the quantities to which the corrections are applied. We also note that the g_J values in Table III are in good agreement with those of Ref. 6.

The corrected values of the hyperfine-interaction constants may now be substituted into Eqs. (10) and (11) to determine the various parameters in Hamiltonians (3) and (4). Their values (all in MHz) are found to be

$$\begin{aligned} a(l) &= -318.3, & a(sC^2) &= -310.1, & a(s) &= 42.1; \\ b^{02} &= 200.9, & b^{13} &= 11.8, & b^{11} &= -5.4; \\ b_{3d} &= 198.0. \end{aligned} \quad (12)$$

The uncertainties in the numbers in Eqs. (12) arise almost entirely from uncertainties in the coefficients in Eqs. (10) and (11); the experimental uncertainties of Table III play only a minor role. Since the set of coefficients depends on the model assumed, it is hard to estimate the uncertainties in them. We would be reluctant to trust the numbers in Eqs. (12) to better than a few percent.

IV. DISCUSSION

In this section, the hfs parameters (Table IV) for the Hund-rule multiplet of Ni, and similar sets of parameters from experiments with other $3d$ -shell atoms, will be examined from two points of view. The first approach is to examine certain ratios of the orbital, spin-dipole, and quadrupole parameters—which is equivalent to comparing the effective values for the radial operators for the three parts of the Hamiltonian. Then we will compare the contact parameter with that for other atoms in the $3d$ shell and with some theoretical calculations of s -electron densities at the nucleus.

TABLE IV. Values of hfs parameters for the Hund-rule multiplet of each $3d^N 4s^2$ atom. Also shown are several other quantities useful in comparing the predictions of Ref. 11 with experiment. Reference 11 predicts that the ratio $\alpha = a(l)/a(sC^2)$ should be the same for both members in each pair shown in the table. It also predicts that μ_I/μ_N will have one value for atoms with $0 < N < 5$, and a different value for those with $5 < N < 10$, where γ is the ratio $b_{3d}/a(sC^2)$. However, since the Sternheimer correction is not available for all elements, the uncorrected $Q' = Q(1-R)$ is used in place of Q , as explained in the text. The nonrelativistic limit $b_{3d} \approx b^{02}$ has been used where necessary to avoid gaps in the table.

Isotope	No. of $3d$ electrons	$a(l)$ (MHz)	$a(sC^2)$ (MHz)	$a(s)$ (MHz)	α	b_{3d} (MHz)	γ	Q' (b)	μ_I^a (μ_N)	I^a	$\frac{\mu_I \gamma}{Q'I}$
$^{45}\text{Sc}^b$	1	168	148	$-72 \leq a(s) \leq -27$	1.13	-65.5	-0.44	-0.22	4.756	$\frac{7}{2}$	2.72
$^{47}\text{Ti}^c$	2	-56.5	-54.8	10.2	1.032	131.4	-2.40	0.29	-0.7883	$\frac{5}{2}$	2.61
$^{51}\text{V}^d$	3	353.7	322.9	-60.5	1.10	-29.2	-0.090	-0.052	5.149	$\frac{7}{2}$	2.55
^{53}Cr	4										
$^{55}\text{Mn}^e$	5			-72.5					3.444	$\frac{5}{2}$	
$^{57}\text{Fe}^f$	6	76	80.8	-10.8	0.94(3)	0	0	0	0.090	$\frac{1}{2}$...
$^{59}\text{Co}^g$	7	692.3	749.2	-86.0	0.924	488(6)	0.651	0.36	4.62	$\frac{7}{2}$	2.39
$^{61}\text{Ni}^h$	8	-318	-310	42.1	1.026	198	-0.639	0.126	-0.7487	$\frac{3}{2}$	2.53
$^{65}\text{Cu}^i$	9	1210	1179	-221	1.026	-350(50)	-0.30	-0.19	2.382	$\frac{3}{2}$	2.51

^aReference 16.

^bReference 1.

^cReference 2.

^dReference 3.

^eReference 8.

^fReferences 4 and 10.

^gReferences 2 and 5.

^hThis work.

ⁱCalculated from Ref. 7 on the assumption that $\alpha_{\text{Cu}} = \alpha_{\text{Ni}}$.

A. Effective Value of $\langle r^{-3} \rangle$

In the Hamiltonian of Eq. (3), the parameters $a(l)$ and $a(sC^2)$ have the form¹² $\alpha = (2\mu_B \mu_N \mu_I / I) \langle r^{-3} \rangle$, where μ_N is the nuclear magneton and μ_I is the nuclear moment in units of μ_N . The theory of Ref. 12 accommodates configuration interaction by allowing a different correction to $\langle r^{-3} \rangle$ in each term of both the dipole Hamiltonian and the quadrupole Hamiltonian [Eqs. (3), (4), and (7)]. If the results of Table IV are substituted into the ratio

$$\alpha = a(l)/a(sC^2) = \langle r^{-3} \rangle_l / \langle r^{-3} \rangle_{sC^2},$$

the value for the 3F multiplet of Ni I is found to be $\alpha = 1.026$. The departure from unity reflects the differences between the corrections to $\langle r^{-3} \rangle_l$ and $\langle r^{-3} \rangle_{sC^2}$.

Bauche-Arnoult¹¹ has incorporated earlier theoretical work²¹ and considered in detail the corrections to $\langle r^{-3} \rangle$ in each of the parameters $a(l)$, $a(sC^2)$, and b_{3d} in the Hund-rule multiplet. Having arrived at expressions for each of the corrections in terms of various combinations of radial integrals, she then forms the ratio α and notes that in the $3d$ shell the same combinations of integrals enter into the expressions for α for several pairs of elements. Unfortunately, numerical values for the radial integrals were not available, so she was not able to calculate values of α or the corrections. However, Bauche-Arnoult notes that the experimental values of α in Fe I and Co I are equal, as predicted, and

further predicts equality between the values for the pairs Sc and Ti, V and Cr, and Ni and Cu. The recent Sc results obtained by Childs¹ do in fact agree well with Bauche-Arnoult's predictions based on the older Ti results.² Table IV lists all values of α measured to date.

For the nickel-copper pair, Bauche-Arnoult had insufficient data to form an experimental value of α , since only two levels of the Ni multiplet had been measured and the relevant copper multiplet is a doublet. However, using a chain of several ratios, she predicts that the value of α for nickel should be "very close to unity." Our experimental value $\alpha_{\text{Ni}} = 1.026$ is in good agreement with this prediction.

Using our value of α in conjunction with the hyperfine-interaction constants A and B obtained by Fischer⁷ for the $3d^9 4s^2 \ ^2D_{3/2,5/2}$ states of copper, we find the parameters for ^{65}Cu I to be

$$\begin{aligned} a(l) &= 1210 \text{ MHz}, & a(sC^2) &= 1179 \text{ MHz}, \\ a(s) &= -221 \text{ MHz}, & b_{3d} &\approx -350 \text{ MHz}. \end{aligned} \quad (13)$$

Unfortunately, the excitation energy of the 2D multiplet of copper is more than $11\,000 \text{ cm}^{-1}$, so it is at present impractical to measure the off-diagonal hfs as was done¹ for scandium.

Bauche-Arnoult also considers the ratio

$$\gamma = \frac{b_{3d}}{a(sC^2)} = \frac{e^2}{2\mu_B \mu_N} \frac{QI}{\mu_I} \left(\frac{\langle r^{-3} \rangle_b}{\langle r^{-3} \rangle_{sC^2}} \right)$$

TABLE V. Comparison between calculated and experimental electron spin densities for $3d^N 4s^2$ atoms. All quantities are in atomic units. Entries in column 3 are from the work of Bagus, Liu, and Schaefer (Ref. 23, Table I), and those in column 4 are calculated from entries in Table IV of the present work.

Atom	N	χ_{calc}	χ_{expt}	$\chi_{\text{calc}}/\chi_{\text{expt}}$
Sc	1	-0.301	$-0.83 \leq \chi \leq -0.31$	0.36 to 0.97
Ti	2	-0.423	-0.508	0.83
V	3	-0.487	-0.646	0.75
Cr	4	-0.537		
Mn	5	-0.598	-0.826	0.72
Fe	6	-0.648	-0.941	0.69
Co	7	-0.682	-1.02	0.67
Ni	8	-0.726	-1.32	0.55
Cu	9	-0.794	-2.19	0.36

$$\approx 2.46 \frac{QI}{\mu_I} \left(\frac{\langle r^{-3} \rangle_b}{\langle r^{-3} \rangle_{sc^2}} \right). \quad (14)$$

Thus, the quantity $(\mu_I/QI)\gamma$ may be expected to be close to 2.46. She finds that the ratio $\langle r^{-3} \rangle_b / \langle r^{-3} \rangle_{sc^2}$ of the radial factors has the same value for all atoms with up to five electrons in the $3d$ shell, and a different value for all atoms with between six and ten $3d$ electrons. Therefore, within each of these two groupings the ratio

$$\mathcal{R}_{12} = \frac{\mu_I^{(1)}}{Q_1 I_1} \frac{Q_2 I_2}{\mu_I^{(2)}} \left(\frac{\gamma_1}{\gamma_2} \right) \quad (15)$$

should be a constant. However, the value of the quadrupole moment Q usually contains a large uncertainty due to the lack of a calculated value of the Sternheimer correction²² for most of the $3d$ atoms.

B. Contact Interaction and s -Electron Spin Densities

The parameter $a(s)$ in the hyperfine-interaction Hamiltonian (3) expresses the strength of the interaction between the electron spins and the nuclear magnetic moment; its magnitude reflects the effective

value of the electron spin density at the nucleus. This term in the effective Hamiltonian accounts for most of the configuration interaction.¹⁰ The excitations entering into this term are the ones in which s electrons are excited to higher s orbitals ("core-polarization" effects).

Recently the strength of the contact interaction (i. e., the electron spin density at the nucleus) has been calculated²³ by the unrestricted-Hartree-Fock method. The calculation was unrestricted in the sense that different radial wave functions were allowed for electrons in states of the same n and l but different m_s . In these calculations, the spin densities at the nucleus are characterized by a parameter

$$\chi = \frac{4\pi}{S} \langle J=L+S, M_J=J | \sum_i \delta(\mathbf{r}_i) S_{zi} | J=L+S, M_J=J \rangle \\ = \frac{2\pi}{S} |\psi(0)|^2. \quad (16)$$

Table V compares some measured and calculated values of the contact interaction strength for $3d^N 4s^2$ atoms. The calculated strengths are generally smaller than the experimental ones.

V. CONCLUSIONS

We find that our measurement of the hyperfine constants of the 3F_2 state of ${}^{61}\text{Ni}$, in combination with earlier experiments, allows us to make several of the comparisons between different atoms for which Bauche-Arnoult¹¹ makes predictions. The predictions are in general borne out well by our data. We also find that the calculations of Bagus *et al.*²³ predict a smaller strength for the effective contact interaction than is called for by our experiments.

ACKNOWLEDGMENT

One of the authors (B. G.) would like to thank the Wisconsin Alumni Research Foundation for partial support.

[†]Work performed under the auspices of the U. S. Atomic Energy Commission.

*Faculty Research Participant from University of Wisconsin—Parkside, Kenosha, Wisc. 53140.

¹G. Fricke, H. Kopfermann, S. Penselin, and K. Schulpmann, *Z. Physik* **156**, 416 (1959); W. J. Childs, *Phys. Rev. A* **4**, 1767 (1971).

²K. H. Channappa and J. M. Pendlebury, *Proc. Phys. Soc. (London)* **86**, 1145 (1956).

³W. J. Childs and L. S. Goodman, *Phys. Rev.* **156**, 64 (1967); W. J. Childs, *ibid.* **156**, 71 (1967).

⁴W. J. Childs and L. S. Goodman, *Phys. Rev.* **148**, 74 (1966).

⁵D. von Ehrenstein, *Ann. Physik* **7**, 342 (1961); W. J. Childs and L. S. Goodman, *Phys. Rev.* **170**, 50 (1968).

⁶W. J. Childs and L. S. Goodman, *Phys. Rev.* **170**, 136 (1968); W. J. Childs, M. S. Fred, and L. S. Good-

man, *Phys. Rev.* **141**, 44 (1966).

⁷W. Fischer, *Z. Physik* **161**, 89 (1961).

⁸G. K. Woodgate and J. S. Martin, *Proc. Phys. Soc. (London)* **A70**, 485 (1957).

⁹R. Winkler, *Phys. Letters* **23**, 301 (1966).

¹⁰W. J. Childs, *Phys. Rev.* **160**, 9 (1967).

¹¹C. Bauche-Arnoult, *Proc. Roy. Soc. (London)* **A322**, 361 (1971).

¹²P. G. H. Sandars and J. Beck, *Proc. Roy. Soc. (London)* **A289**, 97 (1965).

¹³I. I. Rabi, J. R. Zacharias, S. Millman, and P. Kusch, *Phys. Rev.* **53**, 318 (1938); J. R. Zacharias, *ibid.* **61**, 270 (1942).

¹⁴W. J. Childs, L. S. Goodman, and D. von Ehrenstein, *Phys. Rev.* **132**, 2128 (1963).

¹⁵N. F. Ramsey, *Molecular Beams* (Oxford U. P., New York, 1956), pp. 272 and 277.

¹⁶All values of nuclear spins and dipole moments in this paper are from G. H. Fuller and V. W. Cohen, in *Nuclear Data Tables*, edited by K. Way (Academic, New York, 1969).

¹⁷B. G. Wybourne, *Spectroscopic Properties of Rare Earths* (Interscience, New York, 1965), pp. 148–152.

¹⁸J. Bauche and B. R. Judd, *Proc. Phys. Soc. (London)* **83**, 145 (1964); R. M. Sternheimer, *Phys. Rev.* **86**, 316 (1952); A. J. Freeman and R. E. Watson, *ibid.* **131**, 2566 (1963).

¹⁹W. J. Childs, *Phys. Rev. A* **2**, 1692 (1970).

²⁰B. R. Judd, *J. Math. Phys.* **3**, 557 (1962).

²¹B. R. Judd, *Proc. Phys. Soc. (London)* **83**, 145 (1964); J. Bauche and B. R. Judd, *Ref.* 18.

²²See, for example, R. M. Sternheimer, *Phys. Rev.* **146**, 140 (1966). The correction for copper has been calculated by R. M. Sternheimer [*Phys. Rev.* **164**, 10 (1967)] and by R. M. Sternheimer and R. F. Peierls [*Phys. Rev. A* **3**, 837 (1971)].

²³P. S. Bagus, B. Liu, and H. F. Schaefer, III, *Phys. Rev. A* **2**, 555 (1970). For notation, see also H. F. Schaefer, III, R. A. Klemm, and F. E. Harris, *Phys. Rev.* **176**, 49 (1968).

Use of Multiple Basis Sets in the Brueckner-Goldstone Many-Body Perturbation Theory for Atomic Problems*

T. Ishihara and R. T. Poe†

Physics Department, University of California, Riverside, California 95502

(Received 12 February 1971)

In the Brueckner-Goldstone many-body perturbation theory as applied to atomic calculations, the origin of important higher-order diagrams is associated with the inflexibility of the single basis set upon which the perturbation expansion is normally based. We show that in calculating each diagram one may employ more than one basis set simultaneously. The use of multiple basis sets is identical to the exact inclusion of a large class of important higher-order terms. We give illustrated examples to show where this technique will be of practical importance. This possibility is expected to improve the accuracy and to extend the range of applicability of the Brueckner-Goldstone many-body perturbation-theory approach.

I. INTRODUCTION

Since its first application by Kelly¹ in a calculation of correlation energy for beryllium, the Brueckner-Goldstone (BG) many-body perturbation-theory approach has been extended to a diverse number of atomic calculations, following essentially the same techniques as developed by Kelly. These include hyperfine interaction and other bound atomic properties,² electron-atom scatterings,³ photoionization problems,⁴ and time-dependent perturbations.⁵

These applications showed that the BG approach enjoys certain distinct advantages such as in the physical interpretations of contributing processes involved. The applications also lead one to conclude that the applicability of the method, as in any perturbation method, rests severely on the choice of the basis set upon which the perturbation series is built. Since the BG theory has been formulated in *one* (single-particle) basis set, it is not surprising that this single basis set cannot be the optimum one for all types of applications. For example, in electron-atom scattering it is clear that one basis set simply cannot be simultaneously compatible

with both the asymptotic conditions for the distorted atomic electrons and the scattered electron.

For a particular calculation, a less-than-optimum choice of the basis set will reflect itself by the presence of important higher-order terms. These important higher-order terms are usually difficult to evaluate—some are simply impossible to evaluate. In the past one must resort to some kind of estimation¹ (e.g., geometric-series approximation) for these higher-order terms. The uncertainty incurred is often hard to assess.

In this paper we show that it is possible to use *simultaneously* more than one basis set in evaluating each term in the expansion of a physical quantity of interest. The ordinary simple rule for calculation remains unchanged. The freedom of using more than one basis set enables one to eliminate a diverse number of important-but-troublesome higher-order terms. Thus the possibility of this usage of a multiple basis set is expected to greatly extend the accuracy and the range of applicability of the BG method.

In Sec. II we review the Brueckner-Goldstone perturbation expansions. In Sec. III we formally develop the multiple-basis-set idea. In Sec. IV